Supplement of Nat. Hazards Earth Syst. Sci., 26, 5315–5338, 2026
https://doi.org/10.5194/nhess-26-5315-2026-supplement
© Author(s) 2026. CC BY 4.0 License.



Natural Hazards and Earth System Sciences
Open Access
EGU

Supplement of

Mobility of dry granular flows over contrasting erodible bed materials in laboratory experiments

Katharina Wetterauer et al.

Correspondence to: Katharina Wetterauer (katharina.wetterauer@unibw.de)

The copyright of individual parts of the supplement might differ from the article licence.

S1 Supplementary Figures S1–S8



Figure S1. Frontal views of the deposits from all 12 fine-particle experiments. (a) Quartz bed for the equal-density scenario, (b) glass bed for the low-density scenario, (c) magnetite bed for the high-density scenario, and (d) rough plywood plate for the non-erosive reference scenario. From top to bottom: repetitions 1, 2, and 3. Grid spacing on the runout area corresponds to 20 cm. /f: fine particles; Rep: repetition.

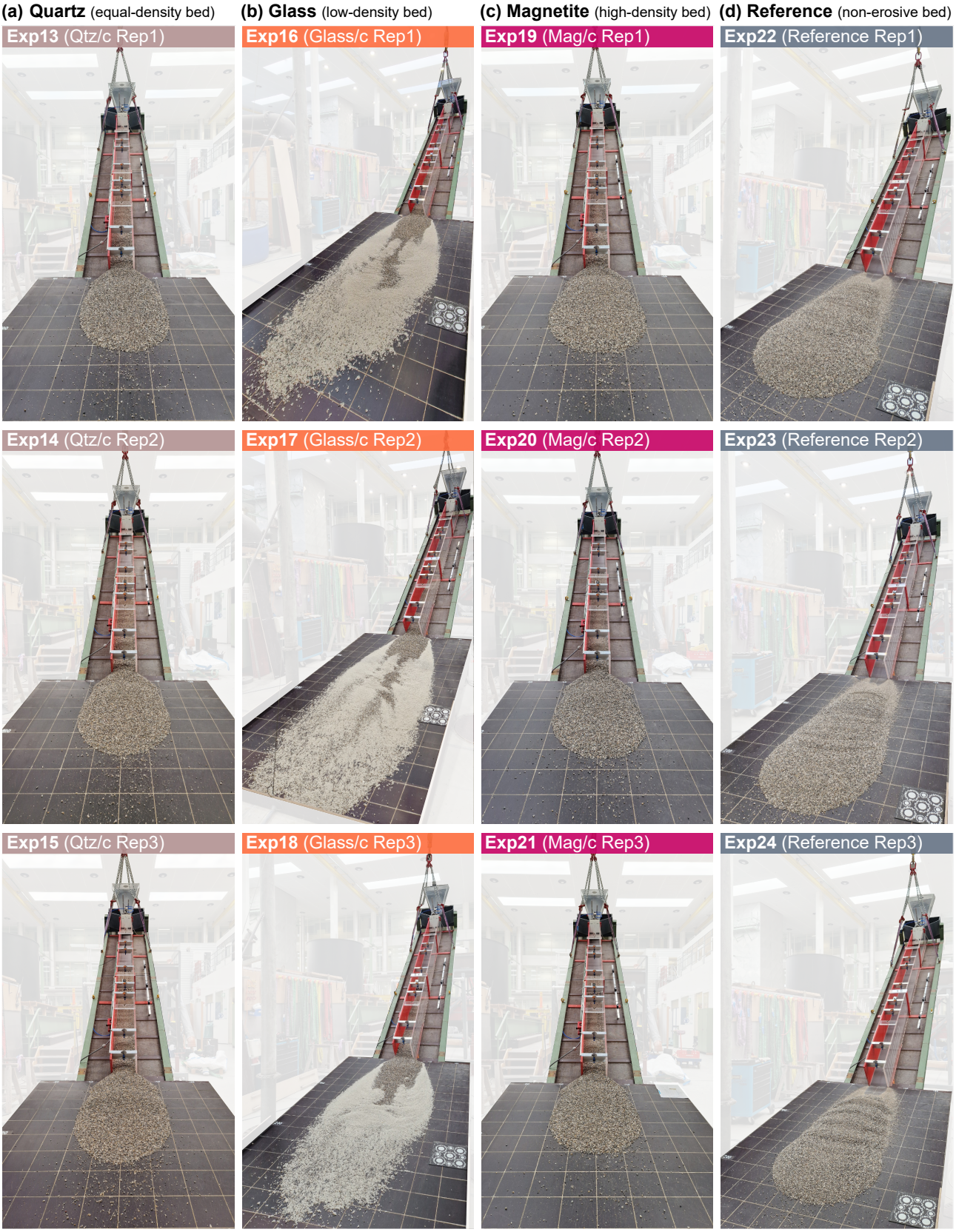


Figure S2. Frontal views of the deposits from all 12 coarse-particle experiments. (a) Quartz bed for the equal-density scenario, (b) glass bed for the low-density scenario, (c) magnetite bed for the high-density scenario, and (d) rough plywood plate for the non-erosive reference scenario. From top to bottom: repetitions 1, 2, and 3. Grid spacing on the runout area corresponds to 20 cm. /c: coarse particles; Rep: repetition.

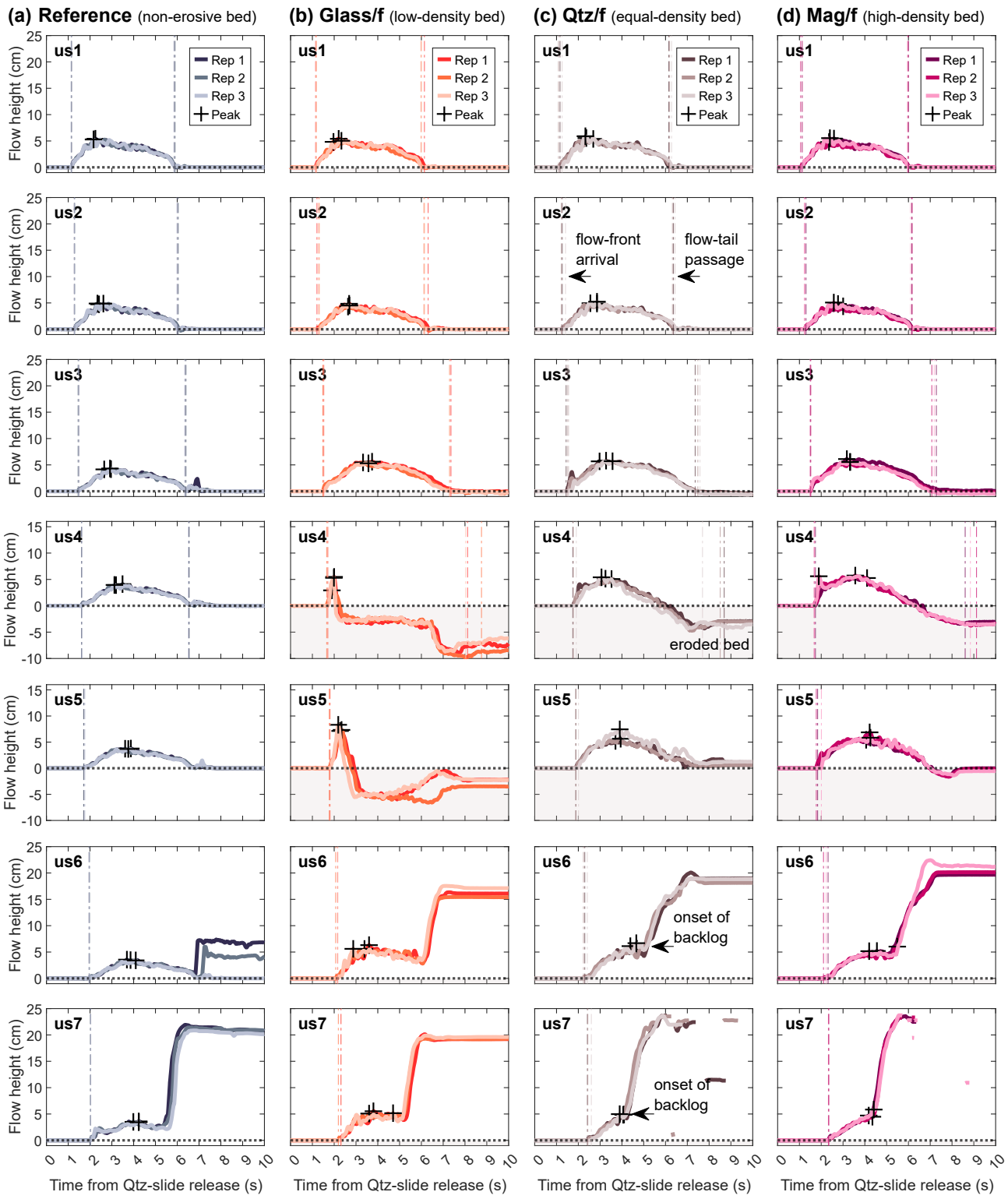


Figure S3. Spatiotemporal evolution of flow height for all 12 fine-particle experiments at all ultrasonic sensors. (a) Non-erosive reference, (b) glass bed, (c) quartz bed, and (d) magnetite bed. From top to bottom: sensor positions us1–us7. Note the strong correspondence among the three repetitions of each scenario. /f: fine particles; Rep: repetition.

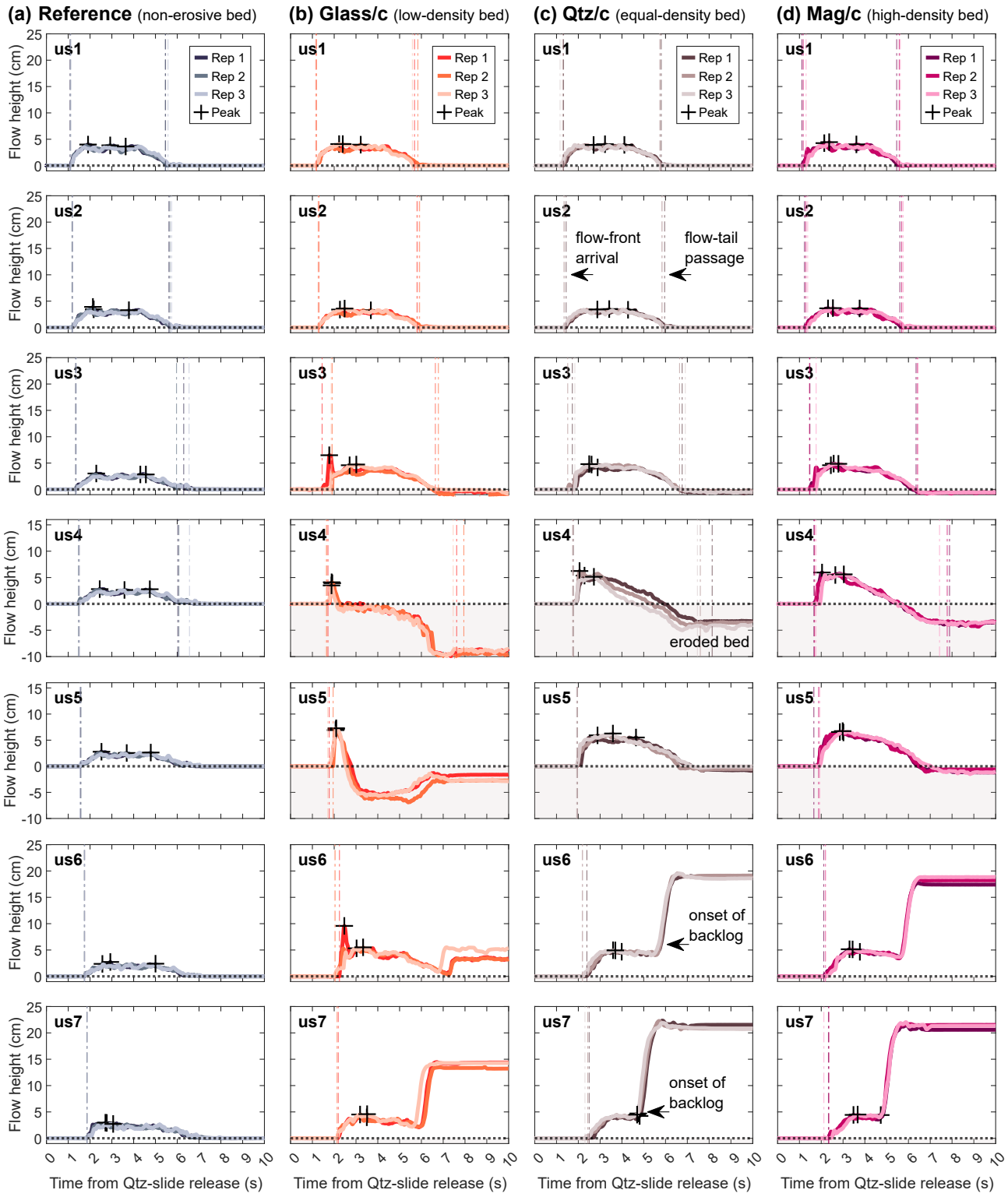


Figure S4. Spatiotemporal evolution of flow height for all 12 coarse-particle experiments at all ultrasonic sensors. (a) Non-erosive reference, (b) glass bed, (c) quartz bed, and (d) magnetite bed. From top to bottom: sensor positions us1–us7. Note the strong correspondence among the three repetitions of each scenario. /c: coarse particles; Rep: repetition.

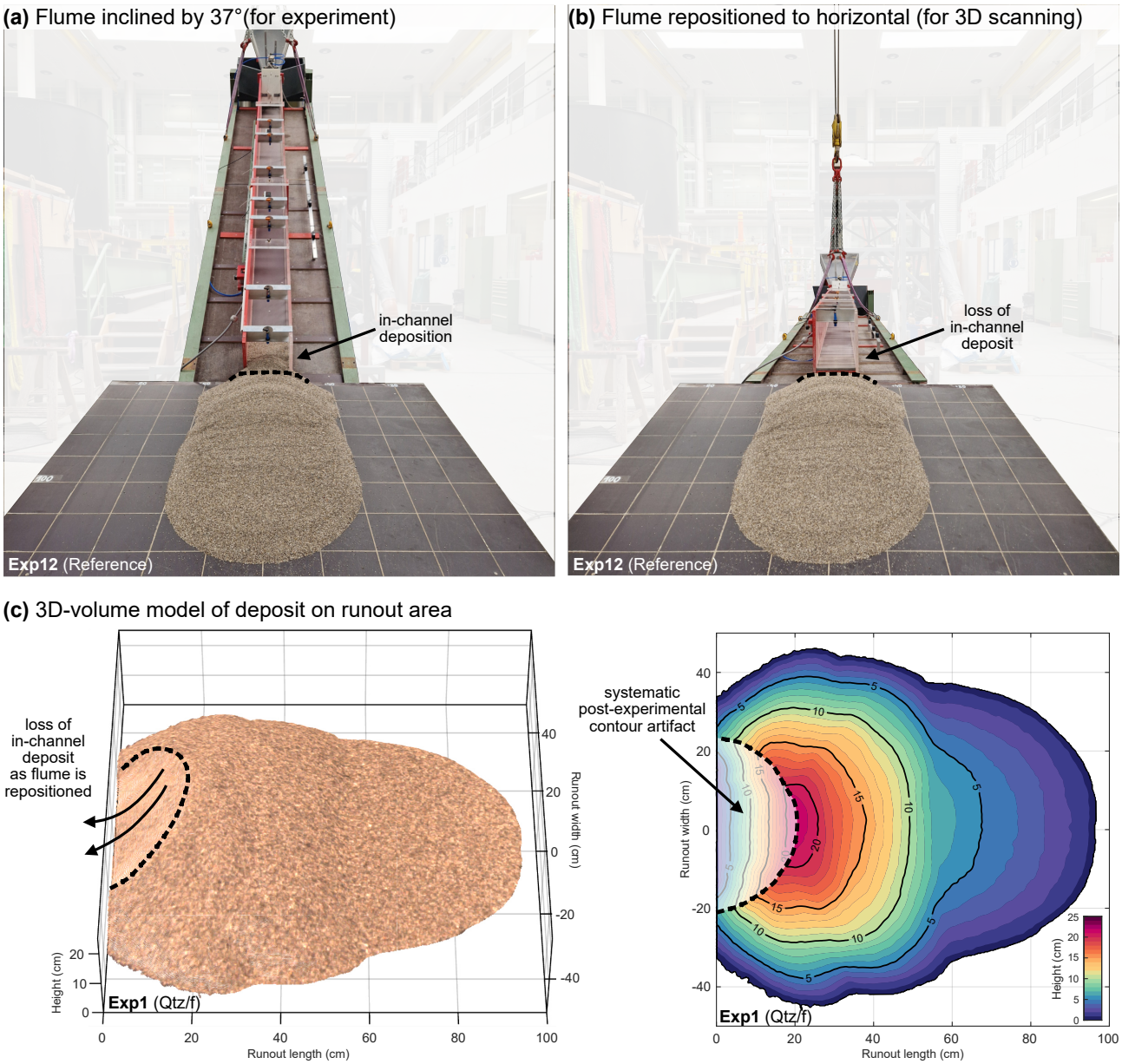


Figure S5. Systematic post-experimental artifacts in the deposits on the runout area caused by in-channel deposition. (a) Flume in the inclined experimental position. (b) Flume repositioned to the horizontal for 3D scanning to avoid reflections from the protruding channel outlet. (c) Morphological artifact in the 3D-volume model at the position corresponding to the channel-outlet location in the inclined setup. Note that photographs and 3D data originate from different experiments, as indicated.

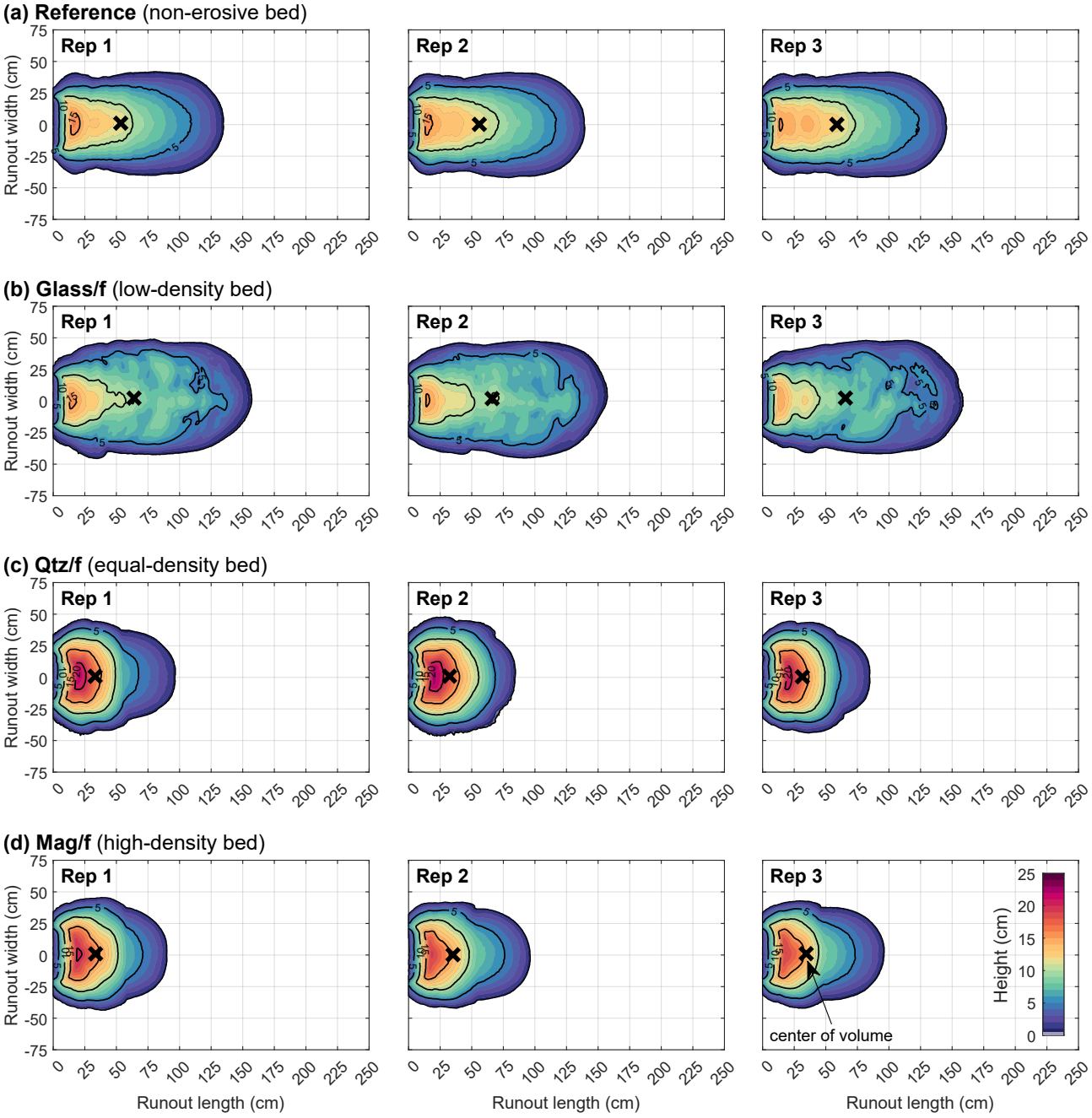


Figure S6. Deposit contour plots for all 12 fine-particle experiments. (a) Non-erosive reference, (b) glass bed, (c) quartz bed, and (d) magnetite bed. From left to right: repetitions 1, 2, and 3. Note the strong correspondence among the three repetitions of each scenario. The flume was repositioned to the horizontal before deposit scanning. Therefore, only material deposited beyond the flume outlet was analyzed, and the apparent thickness drop towards $(0|0)$ is a systematic artifact (see Fig. S5). /f: fine particles; Rep: repetition.

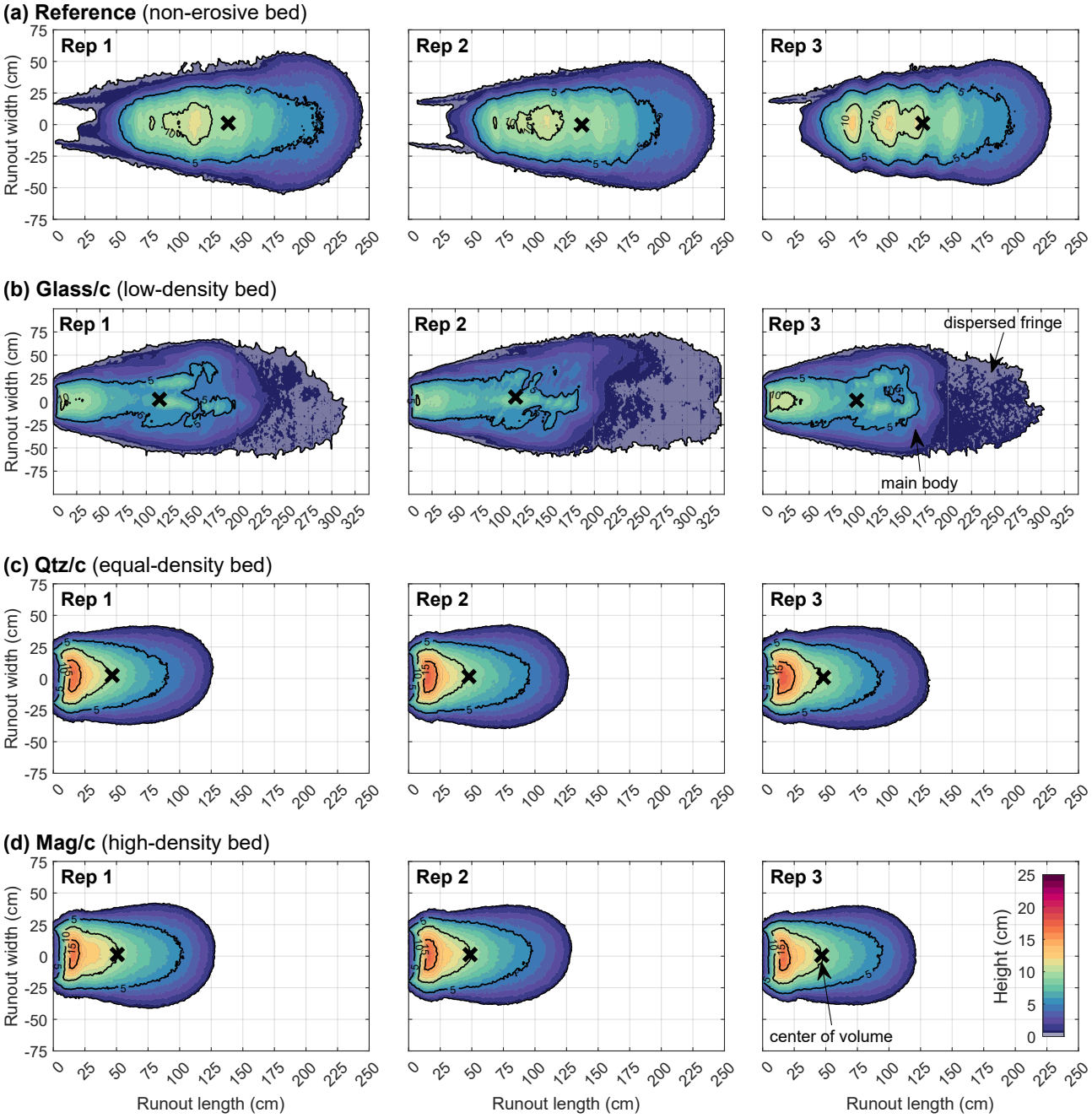


Figure S7. Deposit contour plots for all 12 coarse-particle experiments. (a) Non-erosive reference, (b) glass bed, (c) quartz bed, and (d) magnetite bed. From left to right: repetitions 1, 2, and 3. Note the strong correspondence among the three repetitions of each scenario. The flume was repositioned to the horizontal before deposit scanning. Therefore, only material deposited beyond the flume outlet was analyzed, and the apparent thickness drop towards $(0|0)$ is a systematic artifact (see Fig. S5). /c: coarse particles; Rep: repetition.

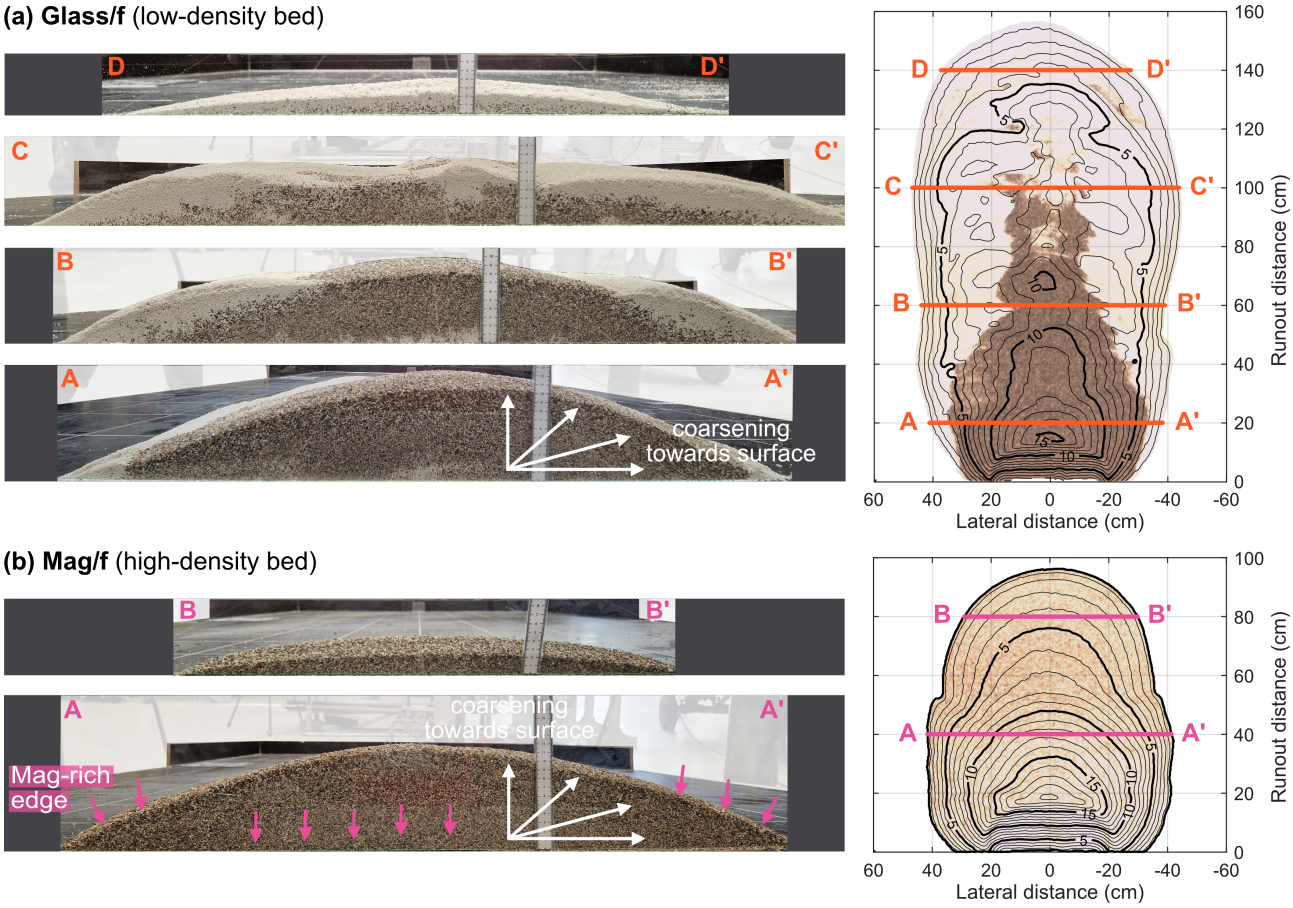


Figure S8. Internal structure and spatial distribution of the (a) Qtz–Glass and (b) Qtz–Mag deposit from fine-particle experiments. Positions of lateral cross sections are indicated on the contoured surface scan. Contour lines are spaced at 1 cm intervals. Note that thicknesses in the cross sections may appear slightly reduced compared to the corresponding contour-plot position, as inserting the glass plate for vertical cutting could drag material downward at the front. Photographs are from Exp5 (Glass/f) and Exp8 (Mag/f).

S2 Supplementary Table S1

Table S1. Reproducibility of the deposits of the four experimental scenarios based on deposit length, deposit width, deposit height, covered area, and deposit volume. Reported are the mean values of the three repeated runs per scenario for fine- (/f) and coarse-particle (/c) experiments together with the corresponding deviation given in absolute units and as percentage deviation from the mean.

Scenario	**Deposit length**			**Deposit width**			**Deposit height**			**Covered area**			**Deposit volume**		
	mean	$\pm 1\sigma$		**mean**	$\pm 1\sigma$		**mean**	$\pm 1\sigma$		**mean**	$\pm 1\sigma$		**mean**	$\pm 1\sigma$	
	(cm)	(cm)	(%)	(cm)	(cm)	(%)	(cm)	(cm)	(%)	(m^2)	(m^2)	(%)	(L)	(L)	(%)
Qtz/f	89	7	8	91	3	3	22	1	3	0.66	0.05	7	53	4	7
Glass/f	158	1	1	92	2	2	15	1	4	1.24	0.01	1	72	4	5
Mag/f	94	3	4	86	3	3	20	1	6	0.67	0.01	1	48	3	5
Reference	140	6	4	83	1	1	16	1	4	1.02	0.06	5	66	6	8
Qtz/c	129	3	2	81	2	3	18	1	3	0.89	0.04	4	49	3	5
Glass/c	318	17	5	130	5	4	11	1	5	3.21	0.38	12	90	1	1
Mag/c	126	4	3	80	2	3	17	0	0	0.87	0.04	4	49	2	4
Reference	238	9	4	106	7	7	12	1	8	1.73	0.19	11	82	1	1